Grant No. NAGW-175

A Photoionization Study of OH and OD from 680Å to 950Å: An Analysis of the Rydberg Series.

J.N. Cutler, Z.X. He and J.A.R. Samson[1]
Department of Physics
University of Nebraska-Lincoln
Lincoln, NE
68588-0111

[1] To whom correspondence should be addressed

Abstract

The photoionization spectra of OH^+ and OD^+ have been reported from 680 to 950Å (18.23 to 13.05 eV) at a wavelength resolution of 0.07Å. Through interpretation of both spectra, the Rydberg series and their higher vibrational members have been reported for three of the excited ionic states, $a^1\Delta$, $A^3\Pi_i$, and $b^1\Sigma^+$. A vibrational progression has also been observed in both OH^+ and OD^+ which is apparently related to a fourth excited ionic state, $c^1\Pi$. Finally, the dissociative ionization limits, corrected to 0 K, for H_2O and D_2O have been measured to be 18.11±0.01 and 18.21±0.01 eV, respectively, and shown to be in good agreement with previously reported results.

I Introduction

Over the past 30 years, the hydroxyl radical (OH) has been one of the most thoroughly studied simple diatomic hydrides due to its importance in atmospheric chemistry[1] and as a component in astrophysical objects (e.g. comet tails)[2,3]. During this time period, OH has been the focus of several different experimental[3-14] and theoretical studies[15-19]. Of particular interest has been a determination of its electronic structure as reflected by its interaction with ultraviolet (UV) and vacuum ultraviolet (VUV) radiation.

Several photoelectron[7-9] and ultraviolet emission[3,4] studies have been completed, but only two previous studies[10,11] have tried to examine the absorption spectra below 1200Å in the VUV region. Viney[10] reported several transitions below 1200Å from the microwave discharge of H_2O which were attributed to the hydroxyl radical. Dehmer[11] later reported a photoionization study of OH from 750 to 950Å in which she states that only modest correlation is found between her work and that of Viney. She attributes Viney's absorption lines to other products such as O_2, H_2, H_2O, etc. which were generated in the microwave discharge. Dehmer assigns only one Rydberg series converging to the $a^1\Delta$ ionization limit.

The ionization potentials for the four lowest ionic states, $X^3\Sigma^-$, $a^1\Delta$, $b^1\Sigma^+$ and $A^3\Pi_i$, have been measured by both photoelectron and ultraviolet emission spectroscopy. In the photoelectron work[7,8], the ionization potentials and vibrational frequencies have been measured for both OH^+ and OD^+. More recently, a pulsed field ionization-zero kinetic energy (PFI-ZEKE) experiment[9] has resolved the rotational structure associated with the lowest ionic state, $X^3\Sigma^-$.

The photoelectron studies have been nicely complemented by the ultraviolet emission experiments of Douglas[4] and later Merer *et al.*[3] This work measured both the molecular constants and ionization potentials of the four lowest ionic states. But until recently, the fifth ionic state, $c^1\Pi$, has not been reported except by theoretical calculations. In a photofragmentation study of OH^+ by Helm *et al.*[12], the apparent $c^1\Pi \leftarrow a^1\Delta$ transition was reported at an energy of 3.53 eV yielding an ionization potential of 18.7 eV for the $c^1\Pi$ state. Insufficient evidence was available to make this a definitive assignment. Later, Rodgers and Sarre[13,14] report the observation of a transition in the $c^1\Pi,\upsilon'=3 \leftarrow b^1\Sigma^+,\upsilon''=0$ with an energy of 2.29 eV. This transition gave an ionization potential of 18.9 eV for the $c^1\Pi,\upsilon'=3$ ionic state agreeing with both theory and the work of Helms *et al.*[12]

In an attempt to better understand OH's VUV features, we have undertaken a high resolution study of OH and its deuterated isotope OD in the energy region from 680 to 950Å (18.23 to 13.05 eV). Our objective is to assign and report the Rydberg series for the different ionic states.

II Experimental

The basic experimental arrangement has been discussed in detail previously[20-22]. Briefly, the radicals of OH and OD were generated by the rapid reaction of atomic hydrogen with nitrogen dioxide, namely[23],

$$NO_2 + H(\text{or } D) \rightarrow OH(\text{or } OD) + NO. \qquad (1)$$

Atomic hydrogen was produced in a microwave discharge by flowing a molecular hydrogen/argon mixture through a Teflon-coated Quartz tube that was surrounded by the

discharge cavity. The flow tube was composed of three concentric tubes. The inner and middle tubes carry the NO_2 and the $H/H_2/Ar$ mixture, respectively. The outer tube was connected to a rotary vane pump to control the flow rate of the reactants. In order to maximize the yield of OH (and OD), the reactants were mixed very near to the ion chamber thereby minimizing loss of product due to contact with walls of the flow tube. The overall efficiency of the reaction was monitored by following the decrease in H^+ signal while adjusting the flow rate of the NO_2. The OH flowed through a 0.5 mm orifice into the interaction region of a magnetic mass spectrometer and was rapidly pumped away by a 170 l s^{-1} turbomolecular pump. The magnetic mass spectrometer, with a mass resolution of 1 in 65, was specifically designed for photoionization studies[24]. The ionization signal was detected with a Galileo Electro-Optic channeltron. At the same time, the incident radiation was monitored with a photomultiplier, coated with sodium salicylate, which was configured in a pulse counting mode. The signals from both the channeltron and photomultiplier were collected by a counter-timer board installed in an IBM PS/2 computer.

The photoionization spectra of OH^+ and OD^+ were recorded at the 1 GeV storage ring Aladdin, located at the Synchrotron Radiation Center in Stoughton, WI. The 4m-Normal Incidence Monochromator was used to cover a spectral region from 680 to 950Å (18.23 to 13.05 eV) at a wavelength resolution of 0.07Å. The wavelength scale was calibrated by using the known Ar $3s^23p^6 \rightarrow$ Ar $3s3p^6\ ^2S\ np'$ and the Ar $3s^23p^6 \rightarrow$ Ar $3s^23p^5\ ^2P_{½}\ ns'$ and $^2P_{½}\ nd'$ autoionizing lines of Ar[25,26] along with the first ionization potential of atomic hydrogen at 911.783Å (13.598 eV)[27]. After the wavelength scale was calibrated,

the peak positions were in excellent agreement with the previous photoionization study of Dehmer[11].

III Results and Discussion

Typical spectra of OH^+ and OD^+ are shown in Figs. 1 and 2. The spectra are composed of numerous autoionizing bands which are superimposed on a continuum background. These autoionizing features are members of different Rydberg series, and their vibrational components, which converge to the different excited state ionization limits of the ion, namely, the $a^1\Delta$, $A^3\Pi_i$, $b^1\Sigma^+$ and $c^1\Pi$ states. The centroids of the most intense manifolds for OH^+ and OD^+ are reported in Table I. A closer examination of one of these bands centered around 13.55 eV, in Fig. 3 and Table II, shows that the broad features in Figs. 1 and 2 are really composed of many sharp rotational lines whose widths (~ 2 meV) are equivalent to our experimental wavelength resolution. These lines are members of P,Q and R branches of a rotational series[28]. In total, the spectra of OH^+ is composed of 414 resolvable peaks and the spectra of OD^+ is made up of 471 peaks. (The peak positions for OH^+ and OD^+ may be obtained from the authors.)

Threshold Region

Figure 4 illustrates the threshold region for both OH^+ and OD^+. The general shape of the two spectra are very similar. The signal begins to increase once the appearance potential is reached, approximately 45 meV below the ionization potential for the $X^3\Sigma^-$ state. The ion signal reaches a maximum after which it falls to the level of a continuum background. A closer examination of Fig. 4 shows that the threshold regions of OH^+ and

OD^+ are more complicated than just a simple threshold step-function onset. The threshold region is convoluted with many rotational bands which manifest themselves as a series of steps in the ionization spectra.

The appearance potentials of OH^+ and OD^+ were measured to be 12.967±0.005 and 12.988±0.005 eV, respectively. In the case of OH^+, our appearance potential is in good agreement with the previous work of Dehmer who reported an onset threshold of 12.96±0.01 eV. The presence of an ion signal below the first ionization potential of the molecule is due to the existence of "rotational hot bands". These "hot bands" will cause the appearance potential to shift to lower energies relative to the adiabatic ionization potential by an amount equal to kT, where T is the rotational temperature of the molecule and k is the Boltzmann constant[29].

More recently, the $X^3\Sigma^- \leftarrow X^2\Pi_i$ threshold photoelectron spectra of OH^+ and OD^+ was obtained by Wiedmann *et al.*[9] using a PFI-ZEKE technique. Due to their overall better experimental resolution, they were able to resolve many rotational lines which are only seen as a series of discreet steps in Fig. 4. The areas of highest rotational line density from Wiedmann *et al.*[9] are plotted against our threshold spectra in Fig. 4. Good correlation is evident between these high line density areas and the steps observed in the threshold spectrum. The arrows in Fig. 4 highlight Wiedmann *et al.*[9] ionization potentials of 13.017 and 13.029 eV for the $X^3\Sigma^-$ ionic state of OH^+ and OD^+, respectively.

Rydberg Series

The spectra of OH^+ and OD^+ are composed of a series of bands which are members of different Rydberg series converging to four different ionic states, $a^1\Delta$, $A^3\Pi_i$,

$b^1\Sigma^+$ and $c^1\Pi$. In the $X^2\Pi_i$ ground state, the electronic configuration of neutral OH is $(2s\sigma)^2(2p\sigma)^2(2p\pi)^3$. However in the ion, the ground state, $X^3\Sigma^-$, and the two excited states, $a^1\Delta$ and $b^1\Sigma^+$, originate from excitation of an electron from the non-bonding ($2p\pi$) molecular orbital. The $A^3\Pi_i$ and $c^1\Pi$ excited states result from excitation of an electron from the bonding ($2p\sigma$) molecular orbital.

In Figs. 1 and 2 along with Tables III-V, three Rydberg series converging to three of the excited ionic states have been identified with the help of known ionization potentials obtained from photoelectron spectroscopy (PES) and by studying the isotope effect on the vibrational frequencies of OH and OD. The quantum defects (δ) and ionization potentials (IP) were determined from the Rydberg equation,[28]

$$E_n = IP - R/(n^*)^2, \qquad (2)$$

where E_n is the energy of the n^{th} member of the Rydberg series, R is the Rydberg constant, and n* is the effective quantum number and is equal to (n-δ). Our instrumental resolution was insufficient to identify the individual Rydberg states with υ=0 and J=0, etc. Thus, the value of E_n was taken at the centroid of the vibrational bands.

In Tables III-V, the centroid position of the vibrational bands, effective quantum numbers, quantum defects, and calculated ionization potentials are reported for three of the observed Rydberg series converging to the $a^1\Delta$, $A^3\Pi_i$ and $b^1\Sigma^+$ states of OH^+ and OD^+.

In the case of the $a^1\Delta$ series for OH^+, the difference between the peaks (see Table III) at 13.555, 14.301, 14.608 and 14.778 gave effective quantum numbers of 2.86, 3.99 and 4.96 along with ionization potentials of 15.218, 15.156 and 15.161 eV, respectively.

These effective quantum numbers and ionization potentials are in good agreement with the previously reported Rydberg series[11] and photoelectron ionization potential of 15.17 eV[8]. A similar series of quantum defects and ionization potentials were obtained for OD^+. The resulting quantum defect (~0.06) infers that the Rydberg series is a member of a *nd*-series which is composed of a series of transitions resulting from the configuration $(2s\sigma)^2(2p\sigma)^2(2p\pi)^2 3d\sigma$, $3d\pi$ and/or $3d\delta$. Based on both dipole selection and angular momentum coupling rules, the $3d\sigma\ ^2\Delta$, $3d\pi\ ^2\Pi$ and $3d\delta\ ^2\Sigma$ states are expected in both the photoabsorption and photoionization spectra[28,30].

In our current experiment, it is not possible to identify the quantum numbers associated with the members of the Rydberg series. Therefore, the quantum defects and quantum numbers reported in Table III could be larger by $n+1$ giving a new quantum defect of ~1. This larger quantum defect would be indicative of a *ns*-series. This inability to distinguish the quantum number connected to a Rydberg series member makes it impossible to explicitly assign the character of the outgoing channel.

Table III relates the position of the $\upsilon'=1$ vibrational members of the $a^1\Delta$ Rydberg series for OH^+ and OD^+. The average vibrational spacing between $\upsilon'=0$ and 1 of 2936 cm^{-1} in OH^+ is in good agreement with the photoelectron value of 2960 cm^{-1}. Franck-Condon calculations by van Lonkhuyzen and de Lange[8] and later by Dehmer[11] showed that the intensity of the OH^+ $a^1\Delta,\upsilon'=1 \leftarrow OH\ X^2\Pi_i\ ,\upsilon''=0$ ionizing transition should be ~20% of the intensity of the main line, $\upsilon'=0 \leftarrow \upsilon''=0$. This small intensity in the $\upsilon'=1 \leftarrow \upsilon''=0$ transition is due to the removal of a non-bonding ($2p\pi$) electron. Figure 5 presents the Morse potential energy curves for the ground state of OH and ionic states of

OH^+. Along with potential energy curves, neutral states that form the Rydberg series converging to the $a^1\Delta$ ionic state are plotted with the limits of the Franck-Condon region. As seen in Fig. 5, there is only a small increase in the bond length when the electron is excited to the higher neutral OH Rydberg states. The maximum Franck-Condon overlap occurs between the lowest vibrational level of the neutral ground state and the lowest vibrational state of the excited Rydberg level. In the spectrum of OD^+, the $\upsilon'=1$ vibrational members are not as immediately evident. A closer examination of Fig. 2 shows that structure is present around positions that are predicted based on the vibrational frequency (see Table III) obtained from the photoelectron spectra[8].

Similar series have been obtained for the $b^1\Sigma^+$ and $A^3\Pi_i$ states which are shown in Figs. 1 and 2 and Tables IV and V. For the $b^1\Sigma^+$ series (see Table IV), four and five members of a Rydberg series for OH^+ and OD^+ were found, respectively. A quantum defect of 0.99 was obtained from the Rydberg series inferring a *ns* nature to the series. The first member of the Rydberg series is unusually weak which may reflect the presence of strong predissocation in this region. In a similar study, Gibson *et al.*[31] reported the photoionization spectrum of SeH^+. They noted that the $b^1\Sigma^+$ Rydberg series had a *ns* nature and the peak intensities were weak due to regions of strong predissociation. An ionization potential of 16.599 eV for OH^+ and 16.607 eV for OD^+ were obtained from the limits of the Rydberg series. These ionization potentials are in good agreement with the PES value of 16.61 eV[8]. The photon energies of the higher Rydberg series members were calculated based on this photoelectron ionization potential.

As seen in the $a^1\Delta$ series, the vibrational member $\upsilon'=1\leftarrow\upsilon''=0$ is only ~20% as intense as the main member of the series due to the removal of a non-bonding ($2p\pi$) electron. The $\upsilon'=1$ vibrational components were not directly observed but calculated positions are disclosed in Table IV based on the vibrational spacing reported by van Lonkhuyzen and de Lange[8]. Autoionizing peaks are observed close to these energies suggesting the presence of the $\upsilon'=1$ member for $b^1\Sigma^+$ Rydberg series.

The $A^3\Pi_i$ series is reported in Table V. For OH^+, a Rydberg series of six members is observed whereas the OD^+ series is composed of only four members. Both series have similar quantum defects, 0.05 for OH^+ and 0.13 for OD^+. These quantum defects are indicative of a *nd*-series. In the SeH^+ paper by Gibson *et al.*[31], two different Rydberg series were observed converging to the $A^3\Pi_i$ ionization limit. The one series was described as a *ns*- or *nd*-series but evidence for a *np*-series was also observed. Due to the bonding nature of the $A^3\Pi_i$ molecular orbital (σ orbital), an effective quantum number reflective of a *np*-series could be observed along with the *ns*- and *nd*-series due to the contribution from the O 2*s*, $2p\sigma$ and H 1*s*. In our study, no evidence of a *np*-series is present. The exact *ns* or *nd* nature of the Rydberg series is impossible to report since the true quantum numbers for the series are could not be determined (see above) . The series limits at 16.474 eV and 16.504 eV for OH^+ and OD^+, respectively, agree well with the PES value for OH^+ of 16.48 eV and for OD^+ of 16.49 eV[8].

Due to the removal of a bonding electron from neutral OH, a long vibrational progression is predicted in the Rydberg series converging to the $A^3\Pi_i$ ionic state (see Fig.

5). In the Franck-Condon calculations of van Lonkhuyzen and de Lange[8] along with Dehmer[11], vibrational intensities of 0.308:0.307:0.194:0.101 are predicted for the υ'=0,1,2,3 vibrational members of this series. In Figs. 1 and 2 and Table V, three members of the vibrational series (υ'=0,1,2) associated with the Rydberg series are reported. The average vibrational splitting for OH^+ of ~2000 cm^{-1} is in good agreement with the photoelectron[8] value of 1960 cm^{-1} and optical spectroscopic[3] value of 1974 cm^{-1}. For OD^+, a average splitting of ~1480 cm^{-1} is measured agreeing with previously values[8,3] of 1469 and 1450 cm^{-1}. The ratio of the vibrational frequencies (from Table V) for OD^+/OH^+ is 0.74. This variation in vibrational spacing between OH^+ and OD^+ is in good accord with the reduced mass of 0.728. In the situations where higher vibrational members could not be observed, peak positions were calculated based on the vibrational frequencies measured from the photoelectron data[8].

A series for the final excited state, $c^1\Pi$, was not observed. However, a vibrational progression in the OH^+ and OD^+ spectra appears above 16.6 eV (see Fig. 6) which may be related to the $c^1\Pi$ state. The vibrational spacing observed in Fig. 6 for OD^+ is about 1100 cm^{-1}. A large vibrational progression is expected since the formation of the $c^1\Pi$ ionic state or the Rydberg series converging to that ionization limit require the excitation or removal of a strongly bonding electron (see Fig. 5). A calculation by Hirst and Guest[15] predicted the vibrational spacing of the $c^1\Pi$ state of OH^+ to be 1727 cm^{-1}. From this, it is possible to calculate a frequency of 1256 cm^{-1} for OD^+. This separation is in reasonable agreement with our data suggesting that the peaks above 16.6 eV are connected to the unobserved $c^1\Pi$ excited state.

Dissociative Photoionization of H_2O and D_2O

The spectra of OH^+ and OD^+ were not continued above ~18 eV due to a rapid increase in the ion signal caused by the formation of OH^+ and OD^+ from the dissociative photoionization of H_2O and D_2O,

$$H_2O + h\nu \rightarrow HO^+ + H + e^-. \quad (3)$$

The onset for dissociative photoionization of H_2O was evidenced by a rapid reasonably linear increase in the ion signal and was found to be 18.07±0.01 eV for H_2O and 18.17±0.01 eV for D_2O. Assuming that the temperature of the molecules is 300 K (3/2 $k\Delta T$=0.039 eV)[29], appearance potentials for dissociative photoionization corrected to 0 K are 18.11±0.01 eV for H_2O and 18.21±0.01 eV for D_2O. These appearance potentials agree very well with the previously reported dissociation limits[32] of 18.115±0.008 and 18.219±0.008 eV for H_2O and D_2O, respectively.

IV Conclusions

In conclusion, the photoionization spectra of OH^+ and OD^+ have been reported at a wavelength resolution of 0.07Å. Through interpretation of both spectra, the Rydberg series and their higher vibrational members have been reported for three of the excited ionic states, $a^1\Delta$, $A^3\Pi_i$, and $b^1\Sigma^+$. A vibrational progression has also been observed in both OH^+ and OD^+ which is apparently related to a fourth excited ionic state, $c^1\Pi$. Finally, the dissociative ionization limits of H_2O and D_2O has been measured and shown to be in good agreement with previously reported results. It is apparent that a great deal more can be

learned about these molecules. Evidence of unresolved rotational structure is tantalizing, but still better resolution is required for a complete analysis of all the rotational features.

Acknowledgments

We would like to thank Dr. M. White for his suggestion on the production of the OH radical and Dr. R. Lipson for his input in the understanding some of the rotational structure. The authors wish to thank the staff at the Synchrotron Radiation Center (Stoughton) for their technical support under NSF Grant No. OMR-9212658. This work is supported by the U.S. National Aeronautics and Space Adminstration under Grant No. NAGW-1751.

References

1. M.J. EcEwan and L.F. Phillips, "Chemistry of the Atmosphere", (Edward Arnold Ltd., London,1977).
2. G.H.F. Diercksen, W.F. Huebner and P.W. Langhoff, "Molecular Astrophysics: State of the Art and Future Directions", (D. Reidel Publishing Co.,Dordrecht,1985).
3. A.J. Merer, D.N. Malm, R.W. Martin, M. Horani and J. Rostas, Can. J. Phys., **53**, 251 (1975) and references therein.
4. A.E. Douglas, Can. J. Phys., **52**, 318 (1974).
5. M.H.W. Gruebele, R.P. Müller and R.J. Saykally, J. Chem. Phys., **84**, 2489 (1986).
6. T.D. Varberg, K.M. Evenson and J.M. Brown, J. Chem. Phys., **100**, 2487 (1994).
7. S. Katsumata and D.R. Lloyd, Chem. Phys. Lett., **45**, 519 (1977).
8. H. van Lonkhuyzen and C.A. de Lange, Mol. Phys., **51**, 551 (1984) and references therein.
9. R.T. Wiedmann, R.G. Tonkyn, M.G. White, K. Wang amd V. McKoy, J. Chem. Phys., **97**, 768 (1992).
10. J.C. Viney, J. Mol. Spectry., **83**, 465 (1980).
11. P.M. Dehmer, Chem. Phys. Lett., **110**, 79 (1984).
12. H. Helm, P.C. Cosby and D.L. Huestis, Phys. Rev. A, **30**, 851 (1984).
13. D.J. Rodgers and P.J. Sarre, Chem. Phys. Lett., **143**, 235 (1988).
14. A.P. Levick, T.E. Masters, D.J. Rodgers, P.J. Sarre and Q.-S. Zhu, Phys. Rev. Lett., **63**, 2216 (1989).
15. D.M. Hirst and M.F. Guest, Mol. Phys., **49**, 1461 (1983).

16. J.A. Stephens and V. McKoy, J. Chem. Phys., **88**, 1737 (1988).

17. M. Merchán, P.-Å. Malmqvist and B.O. Roos, Theor. Chim. Acta., **79**, 81 (1991).

18. R.P. Saxon and B. Liu, J. Chem. Phys., **85**, 2099 (1986).

19. D.R. Yarkony, J. Phys. Chem., **97**, 111 (1993).

20. J.A.R. Samson and P.N. Pareek, Phys. Rev. A, **31**, 1470 (1985).

21. G.C. Angel and J.A.R. Samson, Phys. Rev. A, **38**, 5578 (1988).

22. J.A.R. Samson and G.C. Angel, Phys. Rev. A, **42**, 1307 (1990).

23. F.P. Del Greco and F. Kaufman, Discussions Faraday Soc., **33**, 128 (1962).

24. W. Poshenrieder and P. Warneck, J. Appl. Phys., **37**, 2812 (1966).

25. R.P. Madden, D.L. Ederer and K. Codling, Phys. Rev., **177**, 136 (1969).

26. R.D. Hudson and V.L. Carter, J. Opt. Soc. Am., **58**, 227 (1968).

27. J.L. Franklin, J.G. Dillard, H.M. Rosenstock, J.T. Heron, K.Draxl and F.H. Field, Nat. Stand. Ref. Data Ser., Nat. Bur. Stand. (U.S.), **26** (1969).

28. G. Herzberg, "Molecular Spectra and Molecular Structure", Vol 1. Spectra of Diatomic Molecules (Van Nostrand Reinhold Co, New York, 1950).

29. P.M. Guyon and J. Berkowitz, J. Chem. Phys., **54**, 1814 (1971).

30. P. Bollmark, B. Lindgren and U. Sassenberg, Phys. Scr., **21**, 811 (1980).

31. S.T. Gibson, J.P. Greene and J. Berkowitz, J. Chem. Phys., **85**, 4815 (1896).

32. K.E. McCulloh, Int. J. Mass Spectrom. Ion Phys., **21**, 333 (1976).

Table I: Photon energy for observed peaks in the photoionization spectra of OH and OD and their characterization†. The accuracy in the peak positions is ±0.005 eV.

OH^+				OD^+			
Energy (eV)		Energy (eV)		Energy (eV)		Energy (eV)	
13.031	w	15.918	m	13.071	w	15.860	w
13.105	vw	16.072	s	13.214	vw	15.950	sh
13.178	vw	16.176	m	13.248	vw	15.978	m
13.246	vw	16.283	w	13.365	m	16.068	w
13.455	w	16.343	m	13.510	w	16.127	s
13.555	vs	16.404	w	13.569	vs	16.259	m
13.637	m	16.509	m	13.650	s	16.300	s
13.738	w	16.537	w	13.766	m	16.408	w
13.809	w	16.618	w	13.843	s	16.466	s
13.832	w	16.656	w	13.938	w	16.576	m
13.903	w	16.730	m	13.995	w	16.632	w
13.961	w	16.766	w	14.093	w	16.740	w
14.026	w	16.828	w	14.229	w	16.794	w
14.209	m	16.945	w	14.301	s	16.889	w
14.301	s	17.037	w	14.369	m	16.931	w
14.416	s	17.154	w	14.537	m	17.053	w
14.608	s	17.206	w	14.633	s	17.199	w
14.681	w	17.298	w	14.683	m	17.325	w
14.778	s	17.366	w	14.798	s	17.459	w
14.909	s	17.456	w	14.911	s	17.545	w
15.068	m	17.551	w	15.019	m	17.607	w
15.136	s	17.635	w	15.104	s	17.727	w
15.359	m	17.763	w	15.271	s	17.766	w
15.451	m	17.842	w	15.431	m	17.853	w
15.599	s			15.596	m	17.915	w
15.752	m			15.748	m	18.035	w
15.839	s			15.814	s		

†vw- very weak, w-weak, m-medium, s-strong, vs-very strong, sh-shoulder

Table II: Photon energy for observed peaks in the photoionization spectra of OH and OD and their characterization† for the member of the Rydberg series centered at 13.56 eV converging to $a^1\Delta$ limit. The accuracy in the peak positions is ±0.005 eV.

OH^+		OD^+	
Energy (eV)		Energy (eV)	
13.521	w	13.529	w
13.528	m	13.533	w
13.533	m	13.538	w
13.535	m	13.541	w
13.537	m	13.544	m
13.539	w	13.546	m
13.541	m	13.548	m
13.546	m	13.549	m
13.548	s	13.552	w
13.551	m	13.554	m
13.554	s	13.556	m
13.557	m	13.559	s
13.561	s	13.562	s
13.562	sh	13.564	s
13.565	s	13.567	s
13.571	m	13.570	m
13.573	sh	13.575	sh
13.575	m	13.576	m
13.579	m	13.579	w
13.581	s	13.583	w
13.590	w	13.585	w
		13.587	w
		13.589	sh
		13.591	s
		13.597	w

†vw- very weak, w-weak, m-medium, s-strong, vs-very strong, sh-shoulder

Table III: Assignment of the $(2s\sigma)^2(2p\sigma)^2(2p\pi)^2\ a^1\Delta\ nd \leftarrow (2s\sigma)^2(2p\sigma)^2(2p\pi)^3\ X^2\Pi_i$ Rydberg series converging to OH^+ and OD^+.

Photon Energy (eV)	n	n*	δ	IP (eV)	υ′; Δω, cm^{-1}
OH^+					
13.555	3	2.86	0.14	15.218	
13.903					1; 2807
14.301	4	3.99	0.01	15.156	
14.681					1; 3065
14.608	5	4.96	0.04	15.161	
(14.97)					1; (2960)
14.778	6	[5.89]	[0.11]		
(15.14)					1; (2960)
14.909	7	[7.22]	[-0.22]		
(15.28)					1; (2960)
∞			Avg	15.178	
				(15.17)[i]	
				(15.20)[ii]	
OD^+					
13.569	3	2.88	0.12	15.209	
(13.84)					1; (2178)
14.301	4	3.88	0.12	15.205	
(14.57)					1; (2178)
14.633	5	5.01	-0.01	15.175	
(14.90)					1; (2178)
14.798	6	[5.97]	[0.03]		
(15.07)					1; (2178)
14.911	7	[7.11]	[-0.11]		
(15.18)					1; (2178)
∞			Avg	15.196	
				(15.18)[i]	

[ ] effective quantum number calculated from the photoelectron IP (Ref. 8)
( ) vibrational spacing taken from photoelectron work (Ref. 8)
[i] Reference 8
[ii] Reference 7

Table IV: Assignment of the $(2s\sigma)^2(2p\sigma)^2(2p\pi)^2\ b^1\Sigma^+\ ns \leftarrow (2s\sigma)^2(2p\sigma)^2(2p\pi)^3\ X^2\Pi_i$ Rydberg series converging to OH^+ and OD^+.

Photon Energy (eV)	n	n*	δ	IP (eV)	υ′; Δω, cm-1
OH^+					
13.178	3	2.00	1	16.580	
(13.53)					1; (2821)
15.068	4	2.95	1.05	16.631	
(15.42)					1; (2821)
15.755	5	4.05	0.95	16.585	
(16.11)					1; (2821)
16.072	6	[5.03]	[0.97]		
(16.42)					1; (2821)
∞			Avg	16.599	
				(16.61)[i]	
				(16.61)[ii]	
OD^+					
13.214	3	2.00	1	16.616	
(13.47)					1; (2086)
15.104	4	3.03	0.97	16.586	
(15.36)					1; (2086)
15.748	5	3.95	0.95	16.620	
(16.01)					1; (2086)
16.068	6	[5.01]	[0.99]		
(16.33)					1; (2086)
16.259	7	[6.23]	[0.77]		
(16.52)					1; (2086)
∞			Avg	16.607	
				(16.61)[i]	
				(16.61)[ii]	

[ ] effective quantum number calculated from the photoelectron IP (Ref. 8)
( ) vibrational spacing taken from photoelectron work (Ref. 8)
[i]Reference 8
[ii]Reference 3

Table V: Assignment of the $(2s\sigma)^2(2p\sigma)\,(2p\pi)^3\ A^3\Pi_i\ nd \leftarrow (2s\sigma)^2(2p\sigma)^2(2p\pi)^3\ X^2\Pi_i$ Rydberg series converging to OH^+ and OD^+.

Photon Energy (eV)	n	n*	δ	IP (eV)	υ′; Δω, cm-1
OH^+					
14.909	3	2.95	0.05	16.472	
15.136					1; 1831
15.359					2; 1799
15.599	4	3.94	0.06	16.475	
15.839					1; 1936
16.072					2; 1879
15.918	5	[4.92]	[0.08]		
16.176					1; 2081
16.404					2; 1839
16.072	6	[5.77]	[0.23]		
16.343					1; 2186
16.537					2; 1565
16.176	7	[6.69]	[0.31]		
(16.42)					1; (1960)
(16.66)					2; (1960)
16.283	8	[8.31]	[-0.31]		
(16.53)					1; (1960)
(16.77)					2; (1960)
∞			Avg	16.474	
				(16.48)[i]	
				(16.49)[ii]	
OD^+					
14.911	3	2.96	0.04	16.464	
15.104					1; 1557
15.271					2; 1347
15.596	4	3.79	0.21	16.543	
15.814					1; 1758
15.978					2; 1323
15.950	5	[5.02]	[-0.02]		
16.127					1; 1202
16.300					2; 1395
16.068	6	[5.68]	[0.32]		
16.300					1; 1395
16.466					2; 1339
∞			Avg	16.504	
				(16.49)[i]	
				(16.50)[ii]	

[ ] effective quantum number calculated from the photoelectron IP (Ref. 8)
( ) vibrational spacing taken from photoelectron work (Ref .8)

[i]Reference 8
[ii]Reference 3

Figure Captions

1. Photoionization spectrum of OH^+ taken at a wavelength resolution of 0.07Å. The ●, ■ and ▲ refer to the members of Rydberg series converging to the $a^1\Delta$, $A^3\Pi_i$ and $b^1\Sigma^+$ states, respectively. The dashed line (·····) shows the two higher vibrational components associated with the first member of the $A^3\Pi_i$ Rydberg series.
2. Photoionization spectrum of OD^+ taken at a wavelength resolution of 0.07Å. The ●, ■ and ▲ refer to the members of Rydberg series converging to the $a^1\Delta$, $A^3\Pi_i$ and $b^1\Sigma^+$ states, respectively. The dashed line (·····) shows the two higher vibrational components associated with the first member of the $A^3\Pi_i$ Rydberg series.
3. Photoionization spectra of OH^+ and OD^+ showing the wealth of rotational structure associated with one member of the $a^1\Delta$ Rydberg series.
4. Photoionzation spectra of OH^+ and OD^+ taken near the ionization threshold for the $X^3\Sigma^-$ state. The open rectangles refer to the region of high rotational line density as measured by Wiedmann *et al.*[9] using a PFI-ZEKE technique. The arrows mark the adiabatic ionization potentials of 13.017 eV for OH^+ and 13.029 eV for OD^+.
5. The Morse potential energy curves for the ionic states of OH^+. The solid (———) lines were generated from experimental molecular constants[3,8]. The broken (- - - - -) line was generated from calculations of Hirst and Guest[15]. The dashed (·····) lines show the positions of the Rydberg series converging to the $a^1\Delta$ limit. The hatched area shows the limits of the Franck-Condon region.

6. Photoionization spectra of OH^+ and OD^+ showing the vibrational progression associated with the $c^1\Pi$ ionic state.

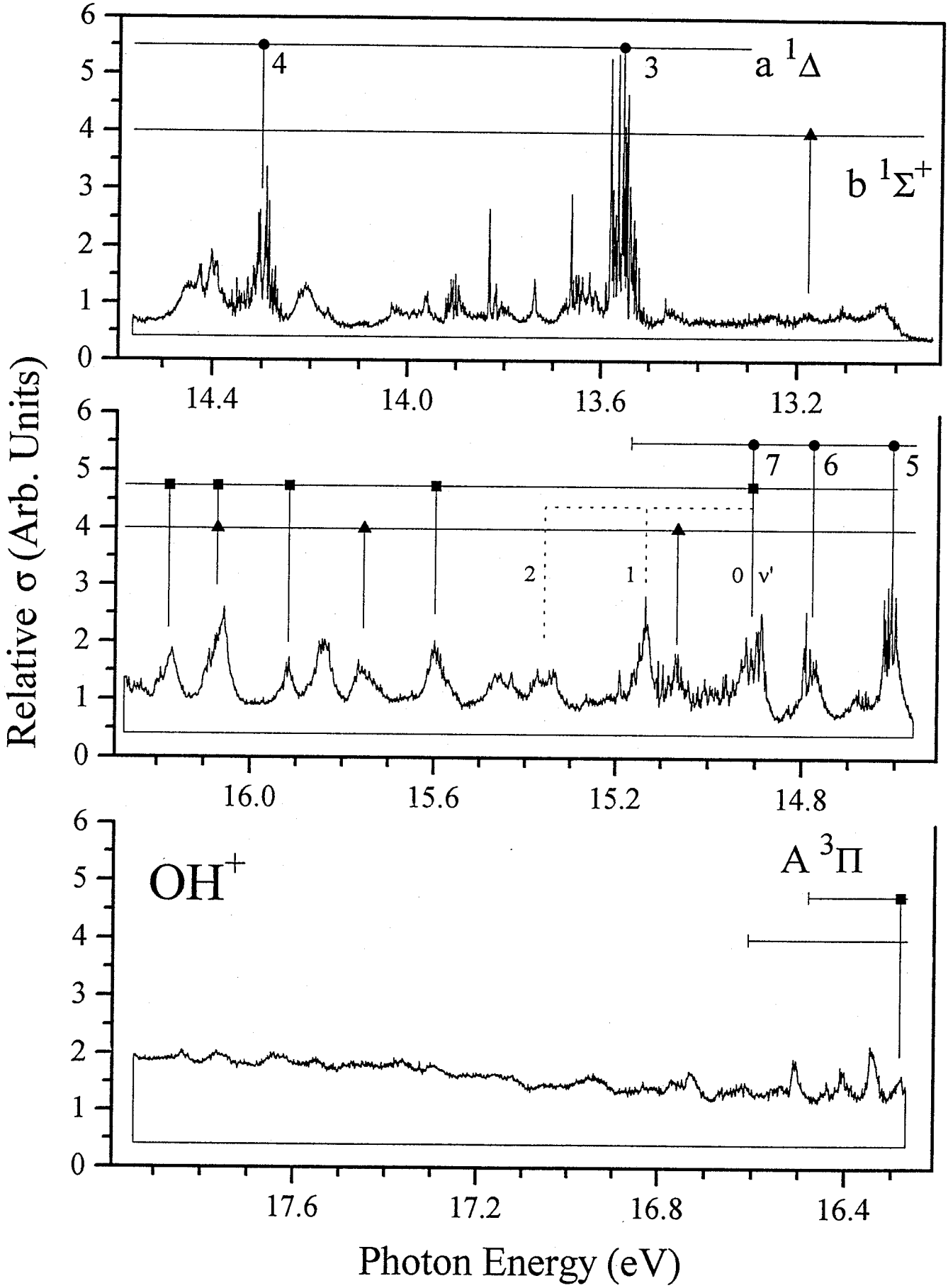
Relative σ (Arb. Units)
Photon Energy (eV)
OH+
a 1Δ
b 1Σ+
A 3Π
4
3
7
6
5
2
1
0
v'
14.4
14.0
13.6
13.2
16.0
15.6
15.2
14.8
17.6
17.2
16.8
16.4

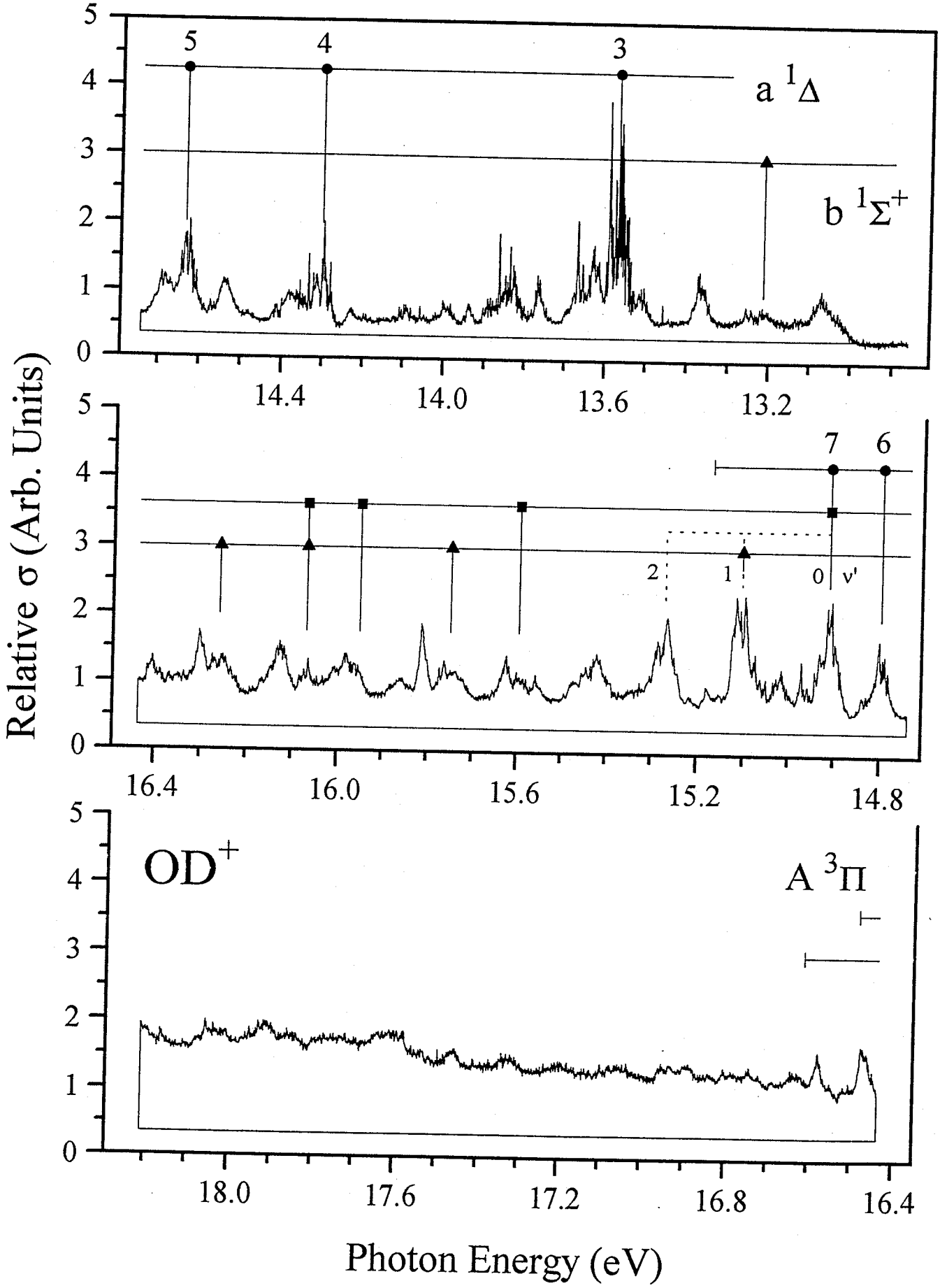
5
4
3
a $^1\Delta$
b $^1\Sigma^+$
14.4
14.0
13.6
13.2
7
6
2
1
0
v'
16.4
16.0
15.6
15.2
14.8
OD$^+$
A $^3\Pi$
18.0
17.6
17.2
16.8
16.4
Relative σ (Arb. Units)
Photon Energy (eV)

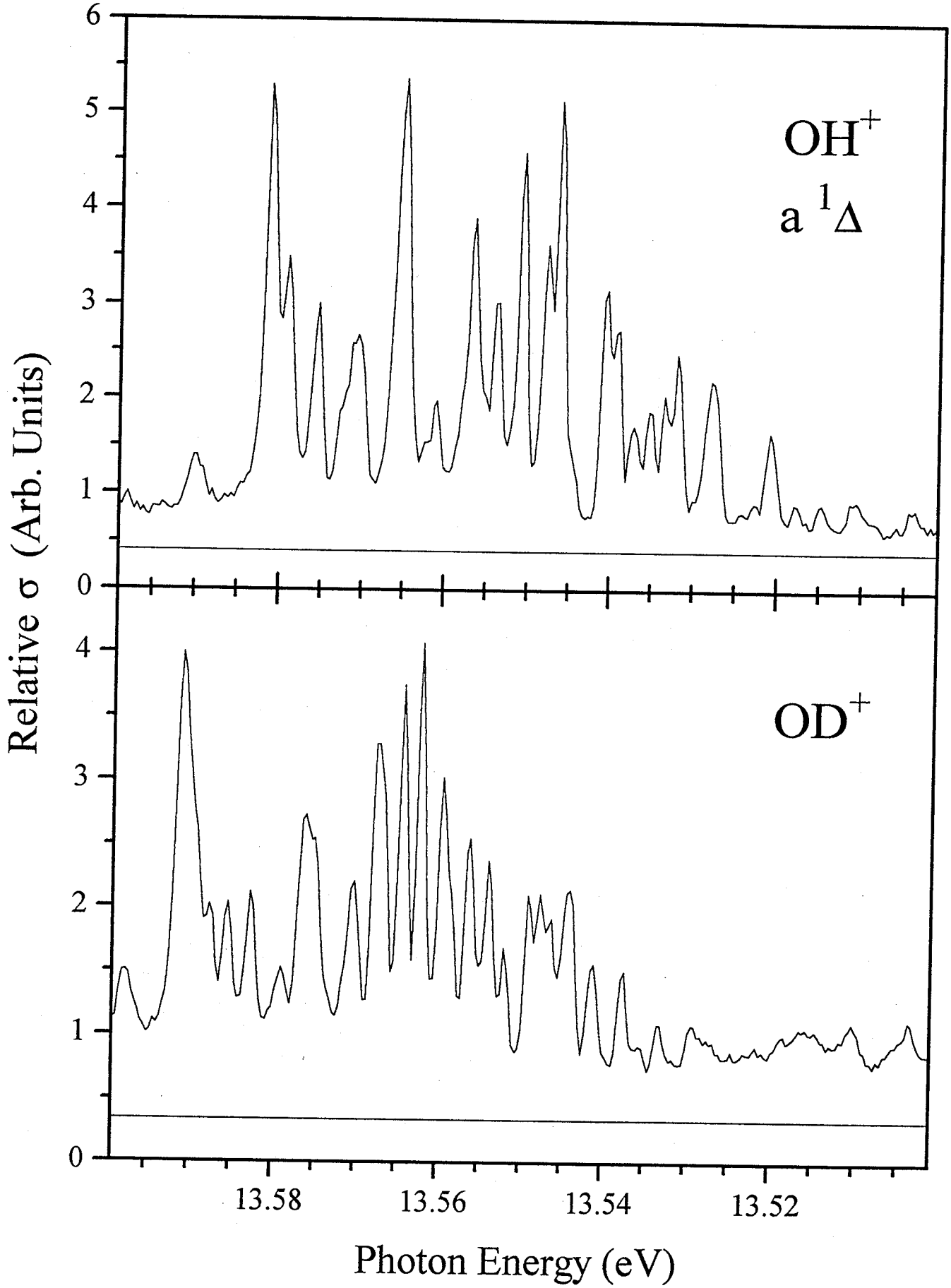
OH+
a 1Δ
OD+
Relative σ (Arb. Units)
Photon Energy (eV)
13.58
13.56
13.54
13.52
0
1
2
3
4
5
6

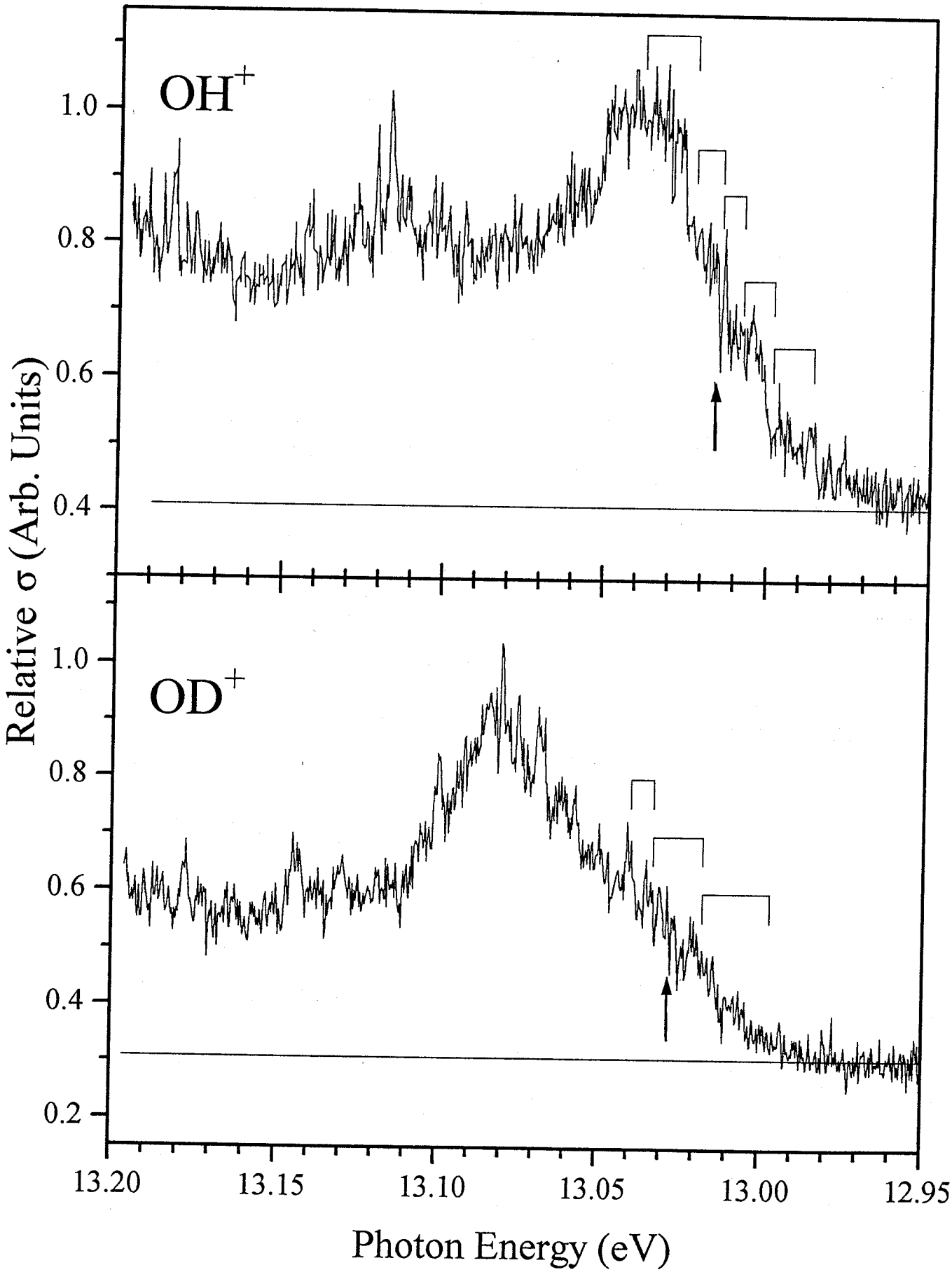
OH+
OD+
1.0
0.8
0.6
0.4
0.2
Relative σ (Arb. Units)
13.20
13.15
13.10
13.05
13.00
12.95
Photon Energy (eV)

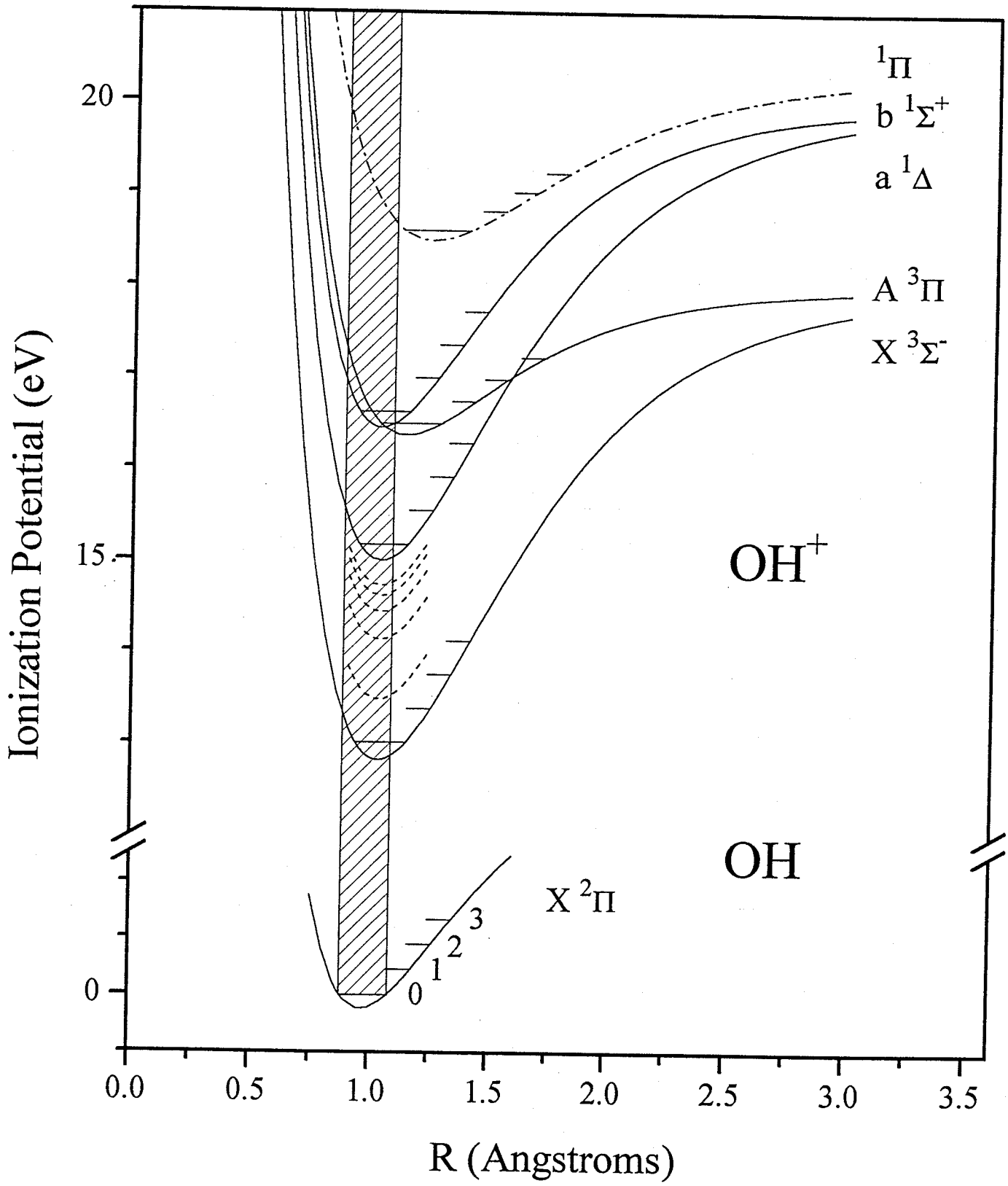
Ionization Potential (eV)
20
15
0
$^1\Pi$
b $^1\Sigma^+$
a $^1\Delta$
A $^3\Pi$
X $^3\Sigma^-$
OH^+
OH
X $^2\Pi$
0
1
2
3
0.0
0.5
1.0
1.5
2.0
2.5
3.0
3.5
R (Angstroms)

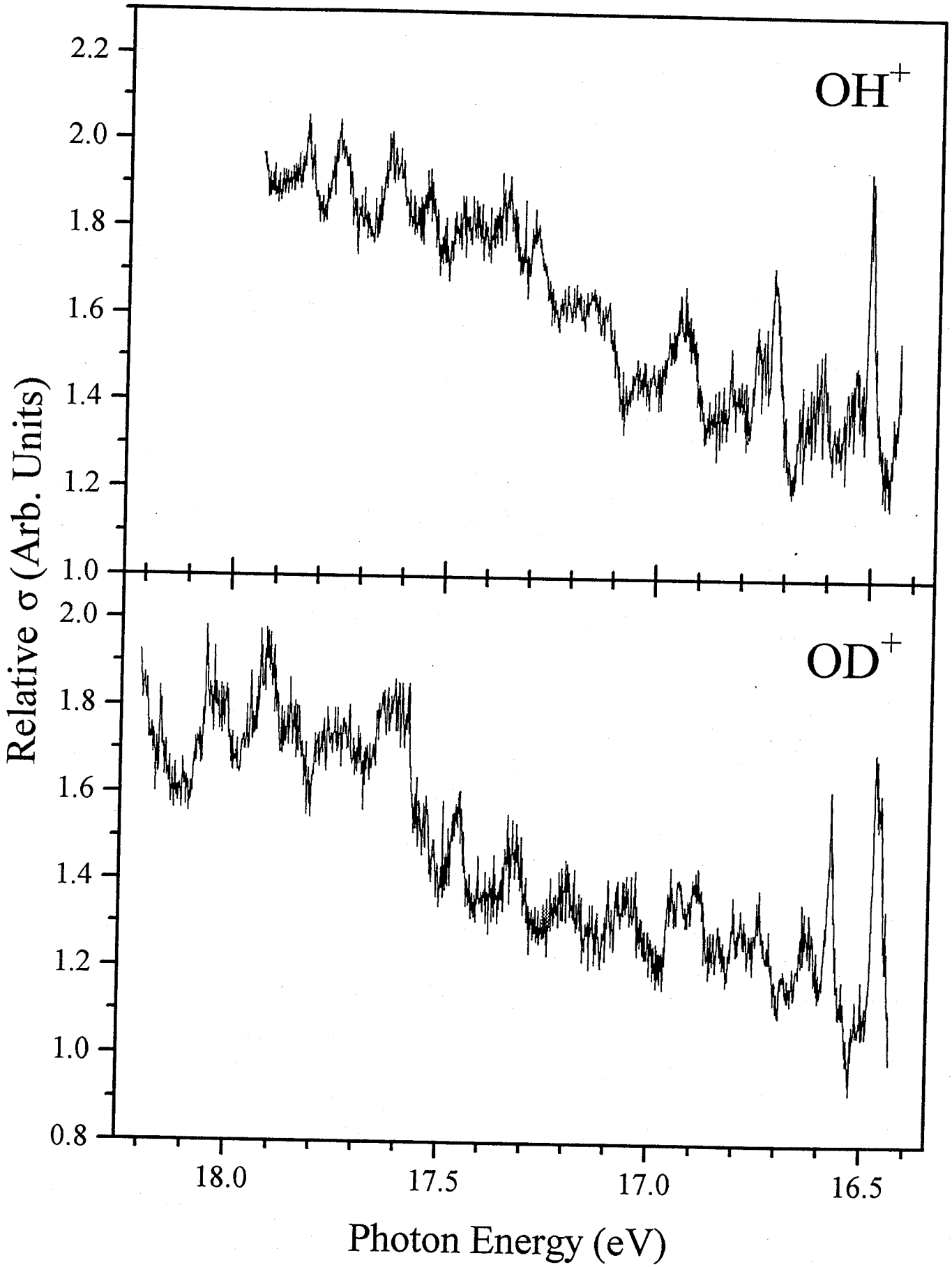
OH+
OD+
Relative σ (Arb. Units)
Photon Energy (eV)
2.2
2.0
1.8
1.6
1.4
1.2
1.0
0.8
18.0
17.5
17.0
16.5